

## CHAPTER IV

### RESULTS AND DISCUSSION

#### 4.1 Characterization of benzoxazine monomers

Phenol derivatives with different functional groups at ortho position were used as starting materials and reacted with methylamine and formaldehyde in order to obtain different functional groups of benzoxazine monomers (see 3.3.1). The products were characterized as follows.

##### 4.1.1 Structural Characterization of 3-methyl-3,4-dihydro-6,8-dimethyl-2H-1,3-benzoxazine (Bm1)

The reaction of 2,4-dimethyl phenol and the solution of formaldehyde with methylamine was completed in 6 hours at 95°C as confirmed by TLC and FTIR. Rate of flow ( $R_f$  value) of 2,4-dimethyl phenol is equal to 0.76 while that of the product is shown at 0.64. The crude product is pale yellow liquid. Further purification by vacuum distillation improved the obtained product to be clear colorless liquid.

Yield : 38.5%

TLC :  $R_f = 0.64$  (ethyl acetate:chloroform = 3:2)

$\rho$  : 1.04 g/cm<sup>3</sup> (at 25°C)

FTIR (ZnSe, cm<sup>-1</sup>) : 1480 (oxazine), 868 (1,2,3,5-substituted), 1258 (C-N stretching), 1287,1120,1031 (C-O-C stretching).

<sup>1</sup>H-NMR (in CDCl<sub>3</sub>, ppm) :  $\delta$ : 2.22 (3H, s, Ar-CH<sub>3</sub>), 2.27 (3H, s, Ar-CH<sub>3</sub>), 2.59 (3H, s, N-CH<sub>3</sub>), 3.93 (2H, s, Ar-CH<sub>2</sub>-N),

4.82 (2H, s, O-CH<sub>2</sub>-N), 6.65 (1H, s, Ar-H), 6.86 (1H, s, Ar-H).

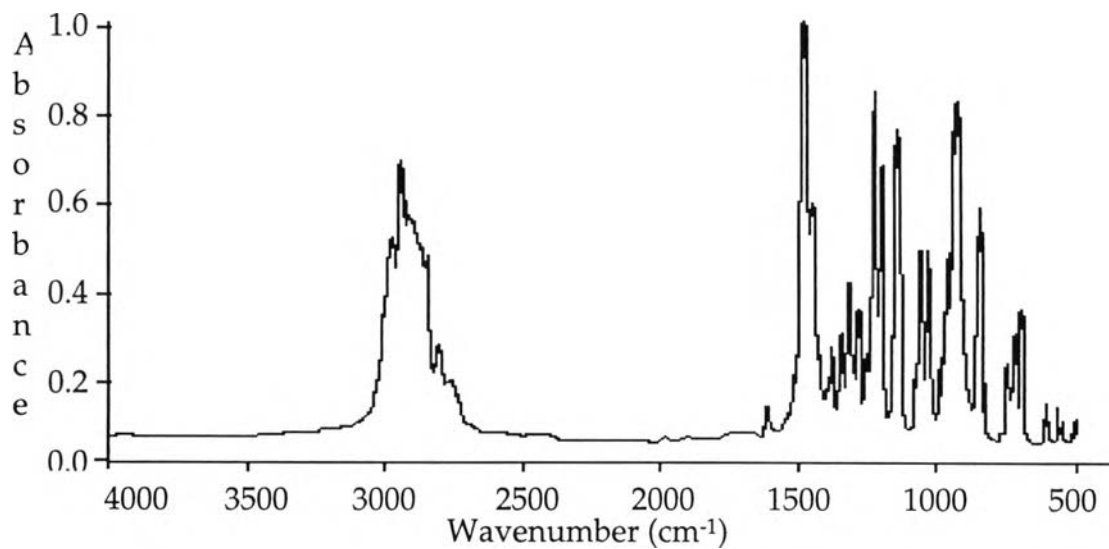


**Figure 4.1** FTIR spectrum of Bm1.

The FTIR spectrum of the synthesized product shows the characteristic peaks of 1,2,3,5-substituted aromatic ring between 860-880 cm<sup>-1</sup> and oxazine linkage at 1480 cm<sup>-1</sup>. The spectrum also shows C-N and C-O-C stretching at 1258 and 1120 cm<sup>-1</sup>, respectively.

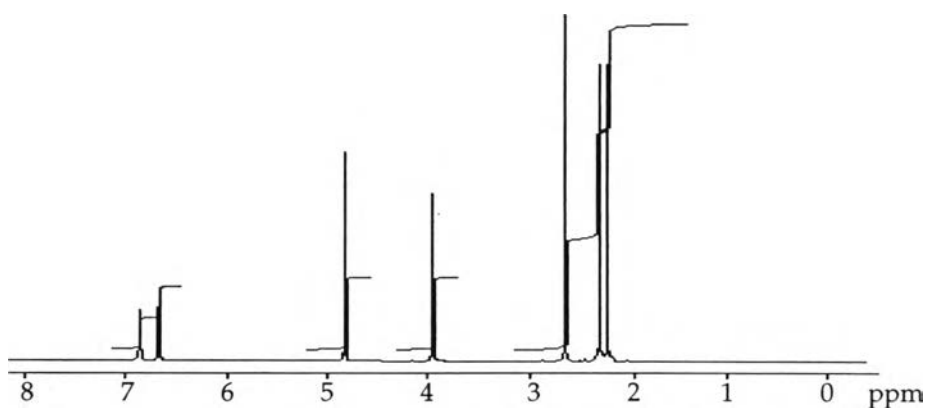


**Figure 4.2** <sup>1</sup>H-NMR spectrum of Bm1.

Figures 4.2 and 4.3 show  $^1\text{H-NMR}$  and  $^{13}\text{C-NMR}$  spectra of the purified benzoxazine (Bm1), respectively. The structure of Bm1 is also confirmed by  $^1\text{H-NMR}$  spectrum which shows the peak position for methyl groups at benzene ring (C-8) around 2.2 ppm and at N-3 for 2.6 ppm. The resonances for methylene groups referred to the one between benzene and nitrogen and another between nitrogen and oxygen occurred at 3.93 ppm and 4.82 ppm, respectively. The protons at benzene ring appear around 6.6-6.9 ppm. It should be noted that the spectrum indicates that of the product is high purity.

To confirm the structure of Bm1, the product was also characterized by  $^{13}\text{C-NMR}$  as shown in Figure 4.3 and Table 4.1.

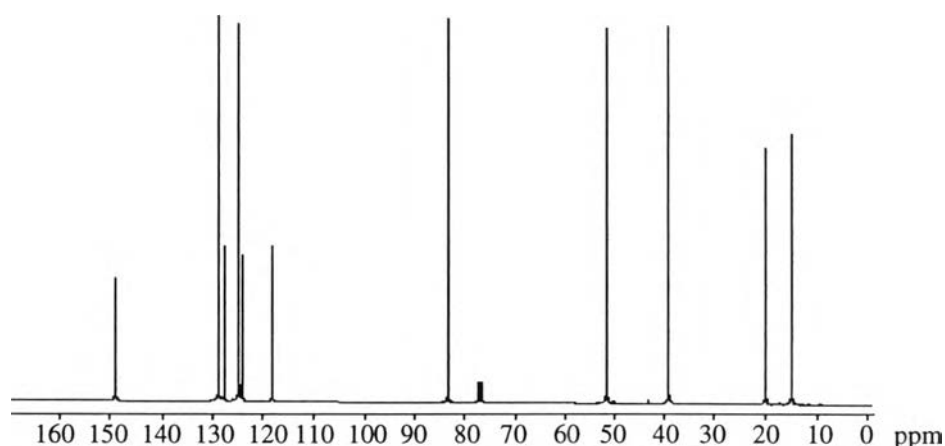


**Figure 4.3**  $^{13}\text{C-NMR}$  spectrum of Bm1.

**Table 4.1**  $^{13}\text{C-NMR}$  Chemical Shifts of Bm1

C-2	N-3(CH <sub>3</sub> )	C-4	C-5	C-6	C-6(CH <sub>3</sub> )	C-7	C-8	C-8(CH <sub>3</sub> )	C-9	C-10
83	39	52	128	118	20	125	124	15	149	129

The  $^{13}\text{C}$ -NMR shows the peak positions corresponding to each carbon in the benzoxazine derivative. Thus, comparing to the work reported by Ishida and Krus (1995), the structure can be concluded as Figure 4.4.

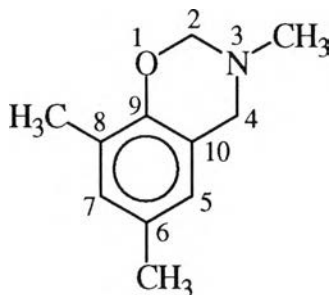


**Figure 4.4 Proposed structure of Bm1.**

#### 4.1.2 Structural Characterization of 3-methyl-3,4-dihydro-6-methyl-8-bromo-2H-1,3-benzoxazine (Bm2)

The difference between Bm1 and Bm2 is that Bm2 has a bromine atom on the ortho position of phenol ring from its starting material instead of methyl group.

To confirm the complete reaction, TLC and FTIR were used. 2-Bromo-4-methyl phenol which was the starting material shows  $R_f$  value for 0.78, while that of crude product is 0.66. The crude product is dark yellowish liquid which can be recrystallized in diethyl ether at room temperature to get the clear colorless cubic crystals. It should be noted that the achieved yield was not good.

Yield : 21%

TLC :  $R_f = 0.66$  (ethyl acetate:chloroform = 3:2)

$\rho$  :  $1.6635 \text{ g/cm}^3$  (at  $25^\circ\text{C}$ )

FTIR (KBr,  $\text{cm}^{-1}$ ) : 1480 (oxazine), 868 (1,2,3,5-substituted), 1258 (C-N stretching), 1287,1120,1031 (C-O-C stretching), 592 (C-Br).

$^1\text{H-NMR}$  (in  $\text{CDCl}_3$ , ppm) :  $\delta$ : 2.19 (3H, s, Ar- $\text{CH}_3$ ), 2.55 (3H, s, N- $\text{CH}_3$ ), 3.87 (2H, s, Ar- $\text{CH}_2\text{-N}$ ), 4.84 (2H, s, O- $\text{CH}_2\text{-N}$ ), 6.68 (1H, s, Ar-H), 7.17(1H, s, Ar-H).

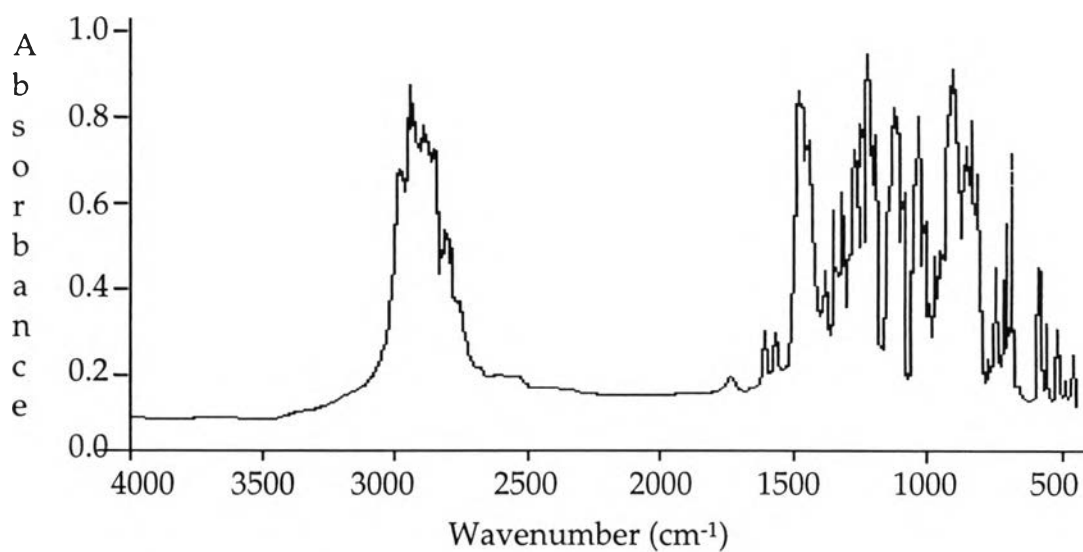


**Figure 4.5 FTIR spectrum of Bm2.**

Bromo derivative gives rise to the C-Br stretching mode at  $592\text{ cm}^{-1}$ . The general appearance of the spectrum is similar to that of Bm1 which can be concluded as the formation of oxazine ring with bromine atom.

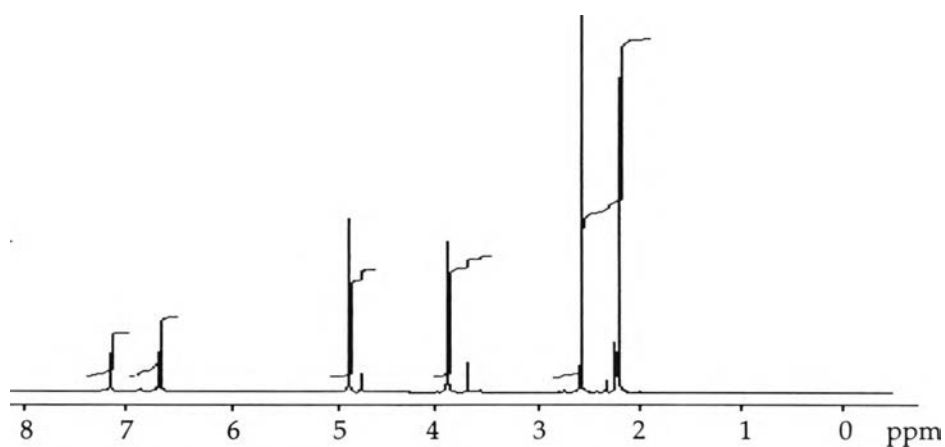


**Figure 4.6  $^1\text{H-NMR}$  spectrum of Bm2.**

The  $^1\text{H-NMR}$  of the product is presented in Figure 4.6. Methyl groups appeared at 2.19 and 2.55 ppm which refers to the ones near aromatic ring and nitrogen atom, respectively. The peak position of methylene groups is similar to that of Bm1. Furthermore, the peak position for the proton on aromatic ring at bromine atom (C-8) is slightly shifted to 7.17 ppm.

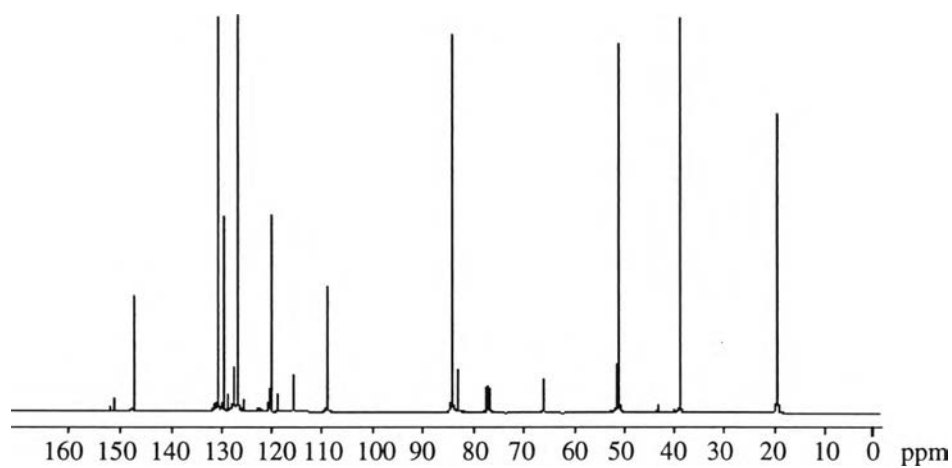


**Figure 4.7**  $^{13}\text{C-NMR}$  spectrum of Bm2.

**Table 4.2**  $^{13}\text{C-NMR}$  Chemical Shifts of Bm2

C-2	N-3(CH <sub>3</sub> )	C-4	C-5	C-6	C-6(CH <sub>3</sub> )	C-7	C-8	C-9	C-10
84	39	51	129	120	20	126	109	147	131

In order to study the molecular weight of the chemical composition of the product, mass spectrometry was applied. As shown in Figure 4.8, the parent peak is observed at  $m/z$  277 which agrees with molecular weight of the product.

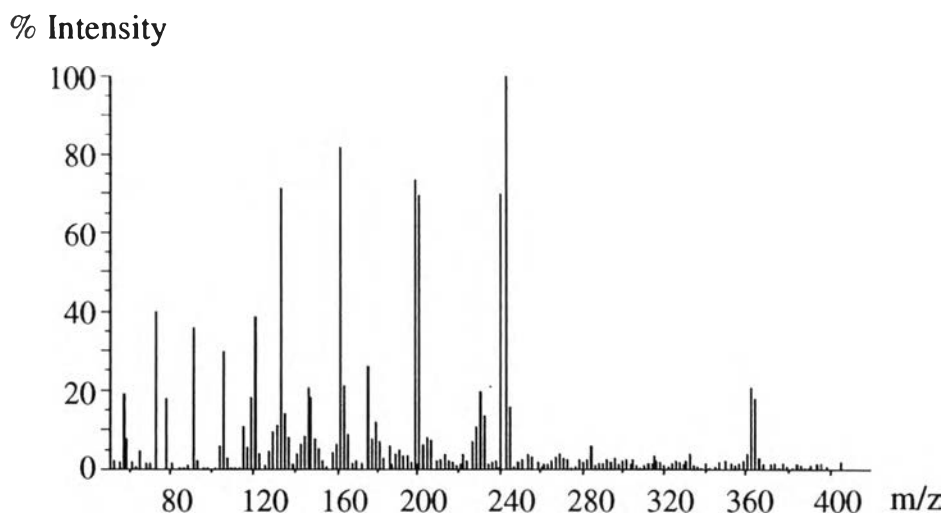


**Figure 4.8 MS spectrum of Bm2.**

As a result, the structure can be proposed in Figure 4.9.

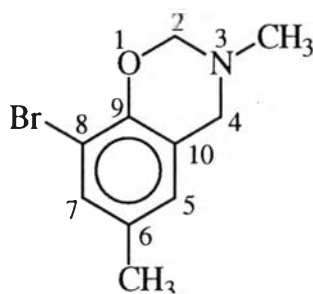


**Figure 4.9 Proposed structure of Bm2.**

#### 4.1.3 Structural Characterization of 3-methyl-3,4-dihydro-6-methyl-2H-1,3-benzoxazine (Bm3)

The starting material, *p*-Cresol, shows  $R_f$  value for 0.74. The reaction was followed by TLC to find  $R_f$  value to be 0.56.

Yield : 63%

TLC :  $R_f = 0.56$  (ethyl acetate:chloroform = 3:2)

$\rho$  : 1.2185 g/cm<sup>3</sup> (at 25°C)

FTIR (KBr,  $\text{cm}^{-1}$ ): 1480 (oxazine), 1258 (C-N stretching), 820,855 (1,2,4 substituted), 1288,1119,1030 (C-O-C)

$^1\text{H-NMR}$  (in  $\text{CDCl}_3$ , ppm): $\delta$ : 2.33 (3H, s, Ar- $\text{CH}_3$ ), 2.68 (3H, s, N- $\text{CH}_3$ ), 4.00 (2H, s, Ar- $\text{CH}_2$ -N), 4.84 (2H, s, O- $\text{CH}_2$ -N), 6.76-6.79 (1H, d, Ar-H), 6.84 (1H, s, Ar-H), 6.98-7.01 (1H, d, Ar-H).

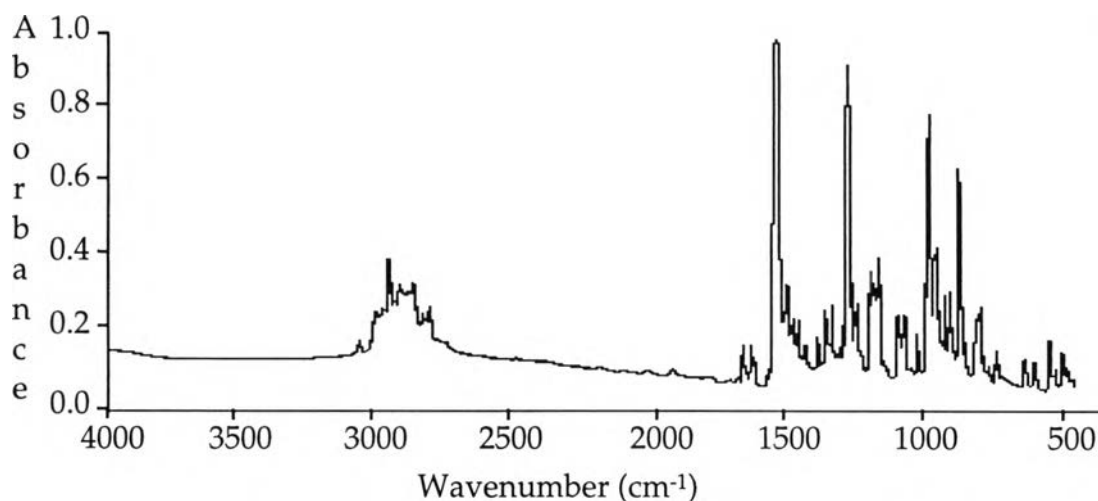


**Figure 4.10** FTIR spectrum of Bm3.

Comparing IR spectrum of Bm1 to Bm3, it is found that the overall peaks are similar. However, the significant band between 860-880  $\text{cm}^{-1}$  which relates to tetra-substituted benzene could not be found, although, the band at 820-860  $\text{cm}^{-1}$ , which is the absorption of tri-substituted benzene, is prominent. It can be concluded that the product is tri-substituted aromatic oxazine ring.



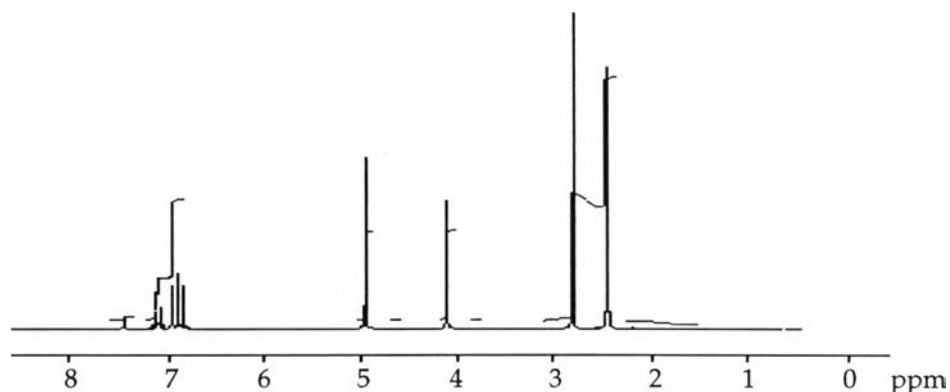


**Figure 4.11** <sup>1</sup>H-NMR spectrum of Bm3.

From <sup>1</sup>H-NMR, The peak positions for protons on aromatic ring are shown as 6.76-6.79 (doublet), 6.84 (singlet) and 6.98-7.01 ppm (doublet), respectively. Among these peaks, the doublet refers to the protons on ortho (C-8) and meta (C-7) position at the same side of benzene ring, while other resonances are slightly shifted comparing to the <sup>1</sup>H-NMR spectra of Bm1 and Bm2. Comparing to the work reported by Burke et al., the structure can be concluded as shown in Figure 4.12.

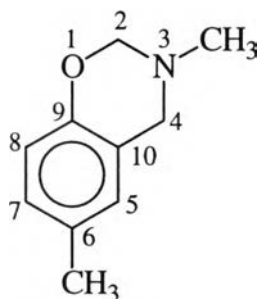


**Figure 4.12** Proposed structure of Bm3.

## 4.2 Ion Extraction Study

By considering the structure of the obtained benzoxazines, it can be expected that benzoxazines give a specific conformation as a host compound to form complexes with some guest molecules. As known for host-guest compounds, when the guest molecules are trapped inside the host cavity, the inclusion phenomena can be observed by analytical techniques, such as ultraviolet spectrophotometry, infrared spectroscopy, atomic absorption spectroscopy, nuclear magnetic resonance spectroscopy, mass spectroscopy, thermal analysis, etc.

Chirachanchai et al. (submitted) demonstrated that oligobenzoxazine and benzoxazine monomer from bisphenol-A showed ion extraction properties of which might be due to molecular assembly. In this work, in order to study the molecular assembly of benzoxazine and its ion entrapment ability, a series of benzoxazine derivatives (Bm1, Bm2, and Bm3) was prepared for comparing ion extraction properties.

Pedersen's technique was applied to study the ion entrapment which can be achieved by the heterogeneous system of water and methylene chloride mixture. However, in the case of Bm2, it was found that the heterogeneous phase of methylene chloride and water became suspension. Thus, in this work Bm2 was not applied for ion extraction study.

In order to clarify the relation between the structure of benzoxazine and ion extraction property, qualitative and quantitative analyses were used. Qualitative analysis was done by using Pedersen's technique while quantitative analysis was studied by titration and atomic absorption techniques to confirm the inclusion phenomena. However, since the present work is the initial step to study the host guest property of benzoxazine, the applied metal ions are limited for alkaline, alkaline earth and other transition metals which can be easily obtained and are not too complicated or dangerous to handle.

#### 4.2.1 Pedersen's Technique

Pedersen's technique is known for the application of ion extraction property in liquid/liquid system study (Pedersen, 1968). Normally, picric acid and metal will form a picrate salt in aqueous phase. The picrate salt will be present in aqueous phase and gives the yellow color to the phase while the organic phase is colorless. Here, the organic phase is favorable for dissolving the host compound and provides the host-guest interaction system which makes the ion shifted to the organic phase as soon as the host-guest compound is formed. The color of the aqueous phase will be changed as the ion is shifted to the organic phase.

In the present work, if the benzoxazine monomer provides a structure as a host molecule and acts as an ionophore, when benzoxazine monomer is added to the system, the metal ions will be shifted to the organic phase as soon as the ion complexes are formed. Thus, the ion extraction can be investigated by determining the change of picrate concentration in the aqueous phase via UV-vis spectrophotometer at the absorption wavelength of the picrate.

The ion extraction for 3-methyl-3,4-dihydro-6,8-dimethyl-2H-1,3-benzoxazine (Bm1) was observed as a function of time. It is found that the extraction percentage increased continuously until achieving the equilibrium state (approximately 15 days) as shown in Figure 4.13.

In order to clarify the structure of benzoxazine in the ion extraction condition, methylene chloride phase was taken to analyze by FTIR using ZnSe cell. It is possible that benzoxazine monomer ring may be opened to form as a dimer, trimer or other oligomers. In this case, the opened structure can be observed as a hydroxyl band around  $3000\text{-}3500\text{ cm}^{-1}$ . However, as confirmed by FTIR, no hydroxyl band was observed for benzoxazine in methylene chloride phase. TLC also shows only one spot ( $R_f = 0.64$ , mobile phase; ethyl acetate/ chloroform =3/2) which reveals that there is only one

component of the compound in the system. Combining these results, it can be mentioned that most of benzoxazine still remained as a Bm1 monomer in ion extraction step. In addition, it is similar to the case of Bm3. It can be concluded that the condition for ion extraction is appropriate for Bm1 and Bm3.

It is likely that the ion extraction phenomena is due to the fact that benzoxazine monomer gradually establishes the molecular assembly for ion guest. Thus, the ion extraction percentage increases according to the extraction time (Figure 4.13).

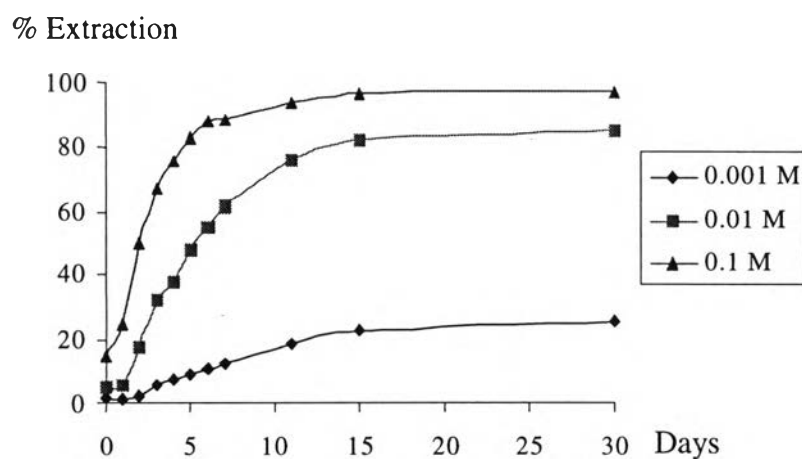


**Figure 4.13** Extraction percentage of lithium picrate, 0.0002 M, in various concentration of Bm1 as a function of time.

Various concentrations of benzoxazine monomer in methylene chloride were applied in order to clarify the capability of benzoxazine as a host compound for ion extraction. Ultraviolet-visible spectrophotometer was used to detect the picrate salt in aqueous phase after achieving the equilibrium state.

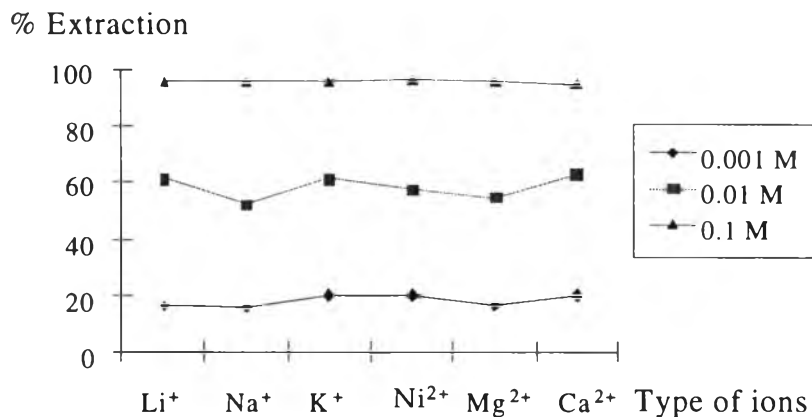


**Figure 4.14** Extraction percentage of metal picrate by Bm1, picrate ion concentration = 0.0002 M.

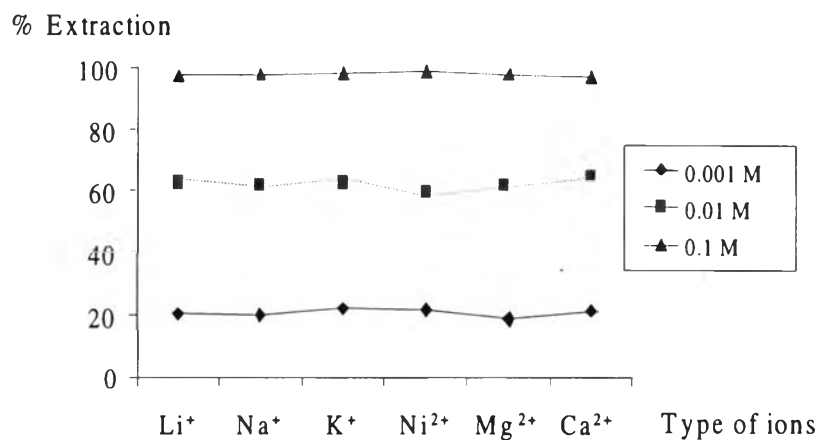


**Figure 4.15** Extraction percentage of metal picrate by Bm3, picrate ion concentration = 0.0002 M.

As summarized in Figure 4.14 and Figure 4.15, it is found that in both cases of benzoxazine monomers, the ion extraction percentage is higher as the benzoxazine concentration is increased. In the case of 0.1 M, the highest concentration in this study, for both monomers, the percentage of ion extraction is nearly 100%. Thus, the ability for ion entrapment of benzoxazine depends on its concentration.

It should be noted that the observed values show no significant change of ion extraction for various types of ions, i.e., less selectivity for ion types. Miyata et al. (1990) reported that when the host molecules form a flexible structure for the guest, various types of guest molecules will be allowed in the cavity. In this study, it should be pointed out that both monomers show high ion affinity but no ion selectivity which may be due to their assembled structures.

However, Bm1 shows slightly higher ion extraction than Bm3. This may be due to the benzoxazine structures of which induced the different assembly structure. This can be confirmed by the fact that Bm1 has a methyl group on the ortho position while there is no functional group at this position for Bm3. The results imply that the steric effect from methyl group causes flexible molecular assembly leading to high ion extraction. Therefore, the difference of ion extraction may be due to the monomer structure and the formation of molecular assembly.

#### 4.2.2 Titration Technique

The inclusion phenomena can be confirmed by titration owing to the following concept.

It is known that picric acid shows very large acidity constant ( $K_a$ ) (Morrison and Boyd, 1959). When the metal ion is added in the system, picric acid will lose its hydrogen atom and form a metal salt complex as shown in step 1 of Figure 4.16. Here, if benzoxazine monomer acts as a host molecule, it will form a complex with picrate salt as shown in step 2 (Figure 4.16). As a result, the pH of the system will be changed owing to the shift of metal ion into organic phase. If the applied metal is hydroxide metal, the pH of the aqueous phase will be lower since the hydroxide and hydrogen are left in the aqueous phase after the movement of picrate salt to the organic phase. In this case, the titration is referred to the addition of benzoxazine monomer solution into the

basic hydroxide metal aqueous phase, which will reduced the pH according to the amount of picrate-benzoxazine complex.

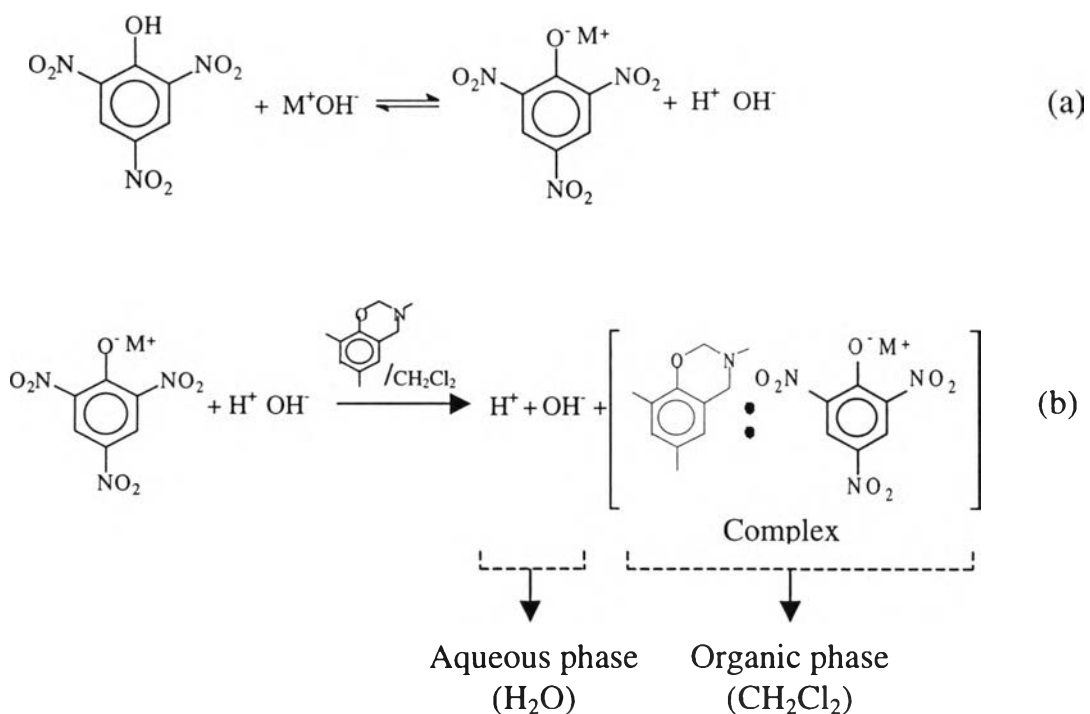


**Figure 4.16** Schematic diagram for 2 steps in titration study (a) step 1: picrate salt formation between picric acid and hydroxide metal species; (b) step 2: complex formation of benzoxazine and picrate salt.

As shown in Figure 4.17, it can be expected that when the ion is formed as a picrate salt, the picrate salt will be shifted to the organic phase after the picrate-benzoxazine complex is formed. Here, the aqueous phase will be neutralized from base (if the applied metal is hydroxide metal), related to the benzoxazine and ion formed as host-guest compound. As a result, the pH of the system will be neutralized according to the less amount of hydroxide metal left in the aqueous phase. The present work applied this concept. The titrating

by benzoxazine solution, which is benzoxazine monomer in methylene chloride, into sodium picrate aqueous solution was done.

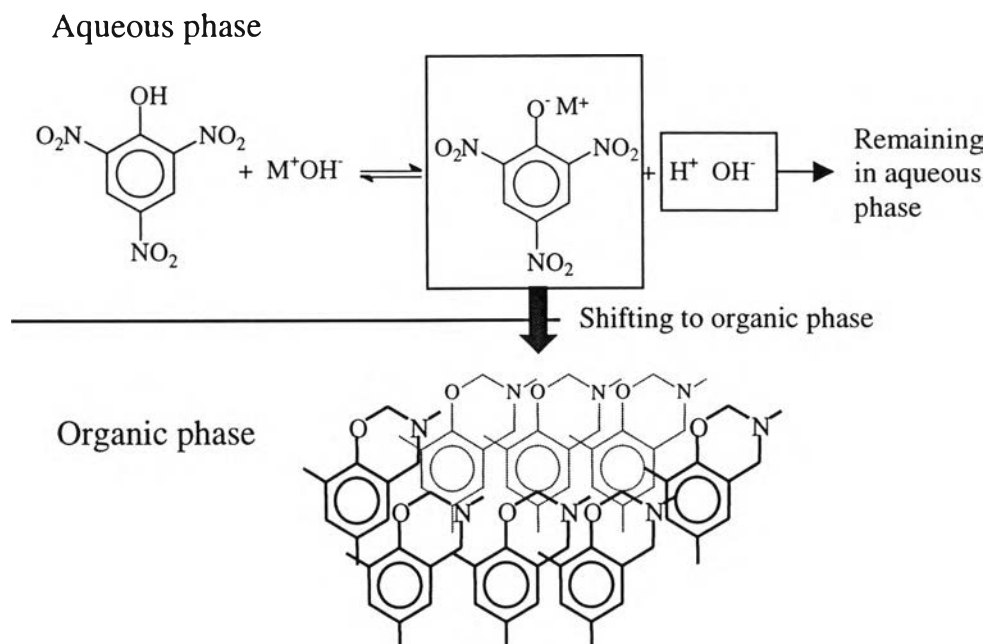


**Figure 4.17 Titration technique for ion entrapment quantitative analysis.**

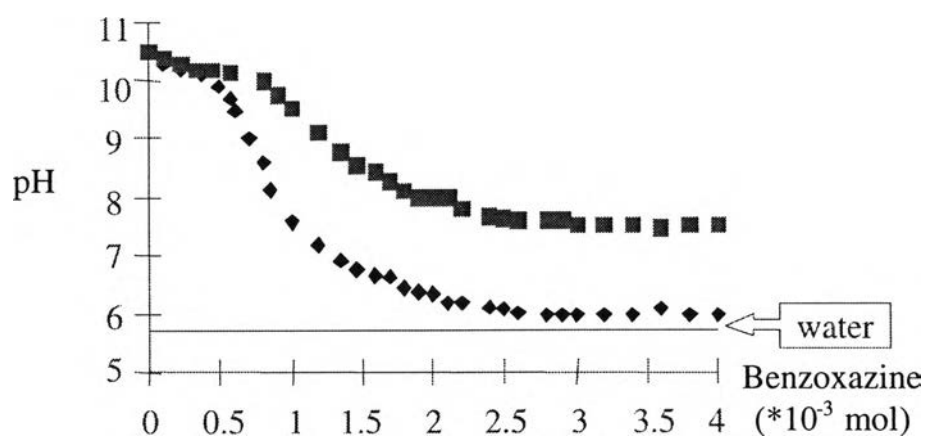


**Figure 4.18 Sodium ion extraction and pH dependence of Bm1 (♦) and Bm3 (■).**

The results indicate that Bm1 reaches the constant pH value at the lower pH than Bm3 (Figure 4.18). This may be explained by the reason that



Bm1 forms host-guest complex with sodium picrate stronger than that of Bm3. Thus, in the system of Bm3, the picrate salt should be left in aqueous phase and the reverse formation to picric acid occurred. As a result, sodium hydroxide is left and induced higher constant pH than water. The result agrees with the one in 4.2.1 which is found that Bm1 can entrap more picrate salt than Bm3. Since the molecular assembly depends on the monomer structure, the steric effect from methyl group should lead to higher flexible assembly and allows the host to perform loose pseudo-cavity or loose packing assembly. The assembly structures of Bm1 and Bm3 can be summarized as shown schematically in Figure 4.19.

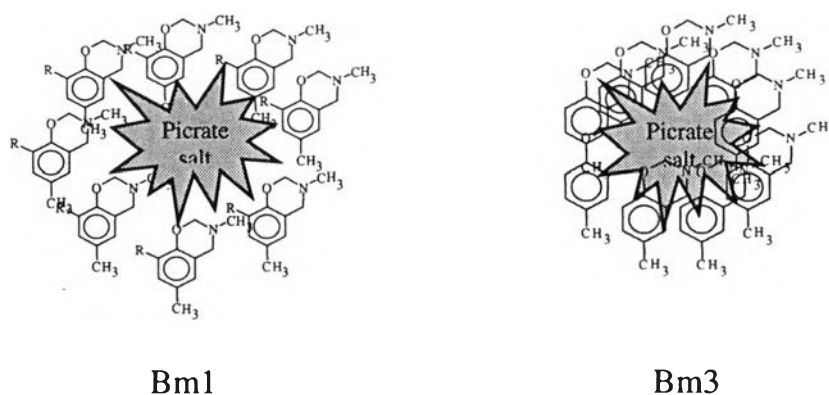


**Figure 4.19** Schematic molecular assembly of Bm1 and Bm3.

#### 4.2.3 Atomic Absorption Technique

Quantitative analysis was also done by atomic absorption spectroscopy. Sodium picrate solution was prepared and shaken vigorously with benzoxazine solution as in the Pedersen's technique experiment. Here, the aqueous phase was separated and the ion concentration was quantified by atomic absorption spectrophotometer according to the method suggested by the manufacturer. It can be expected that the higher the ion is entrapped by the host, the less ion concentration will be observed.

**Table 4.3 Average Sodium Ion Concentration Measured by Atomic Absorption Spectrophotometer (after leaving the mixture for one day)**

Sample	[Na <sup>+</sup> ]/(ppm)
Blank solution*	4.7
After shaking with Bm1**	1.5
After shaking with Bm3**	1.8

\* Sodium picrate solution is 0.0002 M.

\*\* Bm1 and Bm3 concentration are 0.1 M.

As demonstrated in Table 4.3, it is found that the decrease of sodium ion after treating with Bm1 is more significant than that with Bm3, i.e.; [Na<sup>+</sup>] for Bm1 is decreased to 1.5 ppm, while for Bm3 is decreased to 1.8. The concentration of blank solution was found to be 4.7 ppm of which is closed to the calculated value from the preparation step. Comparing the results from Pedersen's and titration techniques (see 4.2.1 and 4.2.2), the ion extraction ability is confirmed to be more significant in the case of Bm1 than that of Bm3.

It is known that the formation of molecular assembly is directly related to the structure of each individual molecule. Bm3 has no bulky group on the benzene ring and the rigid packing assembly structure may be formed and ion extraction can not be achieved efficiently. For Bm1, in another words, the steric hindrance of monomer structure provides the flexible assembly. As a result, the ion extraction ability can be explained as shown in schematic model (Figure 4.19).